

Synthesis, Growth, Spectral and Computational Studies on 6-Aminouracil-1- Methylpyrrolidin-2-One Single Crystal

D. Chandrika^a, R.Santhakumari^{a, *}

^aDepartment of Physics, Government Arts College for Women (Autonomous), Pudukkottai-622 001,
(Affiliated to Bharathidasan university, Tiruchippalli – 620 024), Tamil Nadu, India.

*Corresponding author E-mail Ids: santhasrinithi@yahoo.co.in.

Article Info

Volume 83

Page Number: 157 - 167

Publication Issue:

September-October 2020

Abstract

Organic single crystals of 6-aminouracil-1-methylpyrrolidin-2-one (6AMP) have been synthesized from the aqueous solution using a slow evaporation solution growth process at ambient temperature. Following the growth process, the title compound was carried out to analyze its structural properties by Single-crystal X-ray diffraction (SCXRD). A powder X-ray diffraction (PXRD) pattern was used to observe the lattice planes and phase purity of the grown crystal. The Fourier transform infrared (FTIR) spectral analysis was performed to identify the functional groups present in the compound. The existence of optical transparency was analyzed through the UV-vis-NIR spectrum. Density functional theory calculations with B3LYP/6-311++G(d,p) basis sets were used to find out HOMO-LUMO analysis, Dipole moment, Polarizability, and Hyperpolarizability, Natural bond orbital (NBO), and Mulliken's atomic charges in the gaseous state. Hirshfeld surface analysis was used to study the intermolecular interactions for the grown title compound.

Keywords: Crystal growth, Growth from solution, X-ray diffraction, FTIR, UV-vis-NIR, DFT, Hirshfeld surface analysis.

Article History

Article Received : 4 June 2020

Revised: 18 July 2020

Accepted: 20 August 2020

Publication: 15 September 2020

1.Introduction

Nonlinear optics has a major part in the research as it has wide applications of frequency shifting, optical memory, and optical modulation which are widely used in the areas of telecommunication, signal processing, and optical interconnections[1-2]. Though organic material has the properties of high nonlinear optical responses with the

microscopic origin, flexible to design and produce novel compounds, it would damage due to the poor mechanical and thermal properties during the process. In this perspective, a new class of hybrid crystals of amino acids has emerged as an interesting resource for nonlinear optical applications [3,5]. These amino acid materials take over

both the thermal and mechanical properties of inorganic compounds.

Amino acids and their compounds are organic materials that have been widely used in pharmaceutical and nonlinear optical applications [6-9]. Uracil, one of the five nucleobases is the significant component of nucleic acids and is extensively used in natural products, due to its biological properties [10]. The 6-aminouracil can act as both nucleophiles and electrophiles which has been used in the preparation of heterocyclic frameworks as the parent compound in -, pyrrolo- and pyrimido-pyrimidines [11-13]. Highly efficient chemical synthetic methods were required for the friendly ecosystem providing utmost structural complexity and diversity with low process, structure, and properties [14, 15]. Therefore, in the present work, we report various characterizations for the grown crystal including Powder-XRD, FTIR, UV-absorption studies, such as HOMO and LUMO energies, Hyperpolarizability, NBO, Natural population analysis, and Hershfield analyses were used to aid in the structural property information.

2. Experimental

2.1 Material synthesis and crystal growth

In a typical synthesis, 6-aminouracil (6A) and 1-methylpyrrolidin-2-one (MP) were synthesized using the solvent DMSO in a 1:1 molar ratio. The measured quantity of 6A and MP were dissolved in methanol and water respectively in the magnetic stirrer. After refluxing it for 3h at 100°C, the solution was made to cool gradually till reaching the ambient. Further, the solution was recrystallized and completely dissolved in methanol at 40°C to obtain the homogeneous mixture, and then it was covered in an air-tight container. The solution was kept undisturbed

for the evaporation process and the colorless single crystal was obtained after 20 days. The synthetic structure scheme for the title compound 6-aminouracil-1-methyl pyrrolidin-2-one (6AMP) is given in Figure 1.

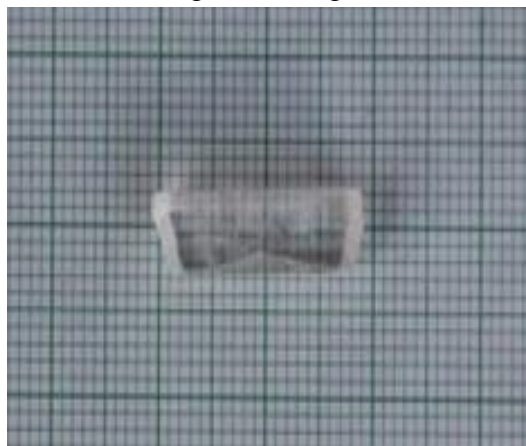


Figure 1. As grown of 6AMP single crystal

3. Results and Discussion

3.1 Powder X-ray diffraction studies

The experimental and the simulated XRD patterns were compared to the reported data for the grown crystal 6AMP from Figure.2. The lattice parameters were calculated for 6AMP as $a = 7.5767(14) \text{ \AA}$, $b = 21.889(3) \text{ \AA}$, $c = 7.1356(11) \text{ \AA}$, $\beta = 117.312(12)$ and volume $V = 1051.49 \text{ \AA}^3$ with space group $P2_1/c$. These values are closely matched with the reported values [16].

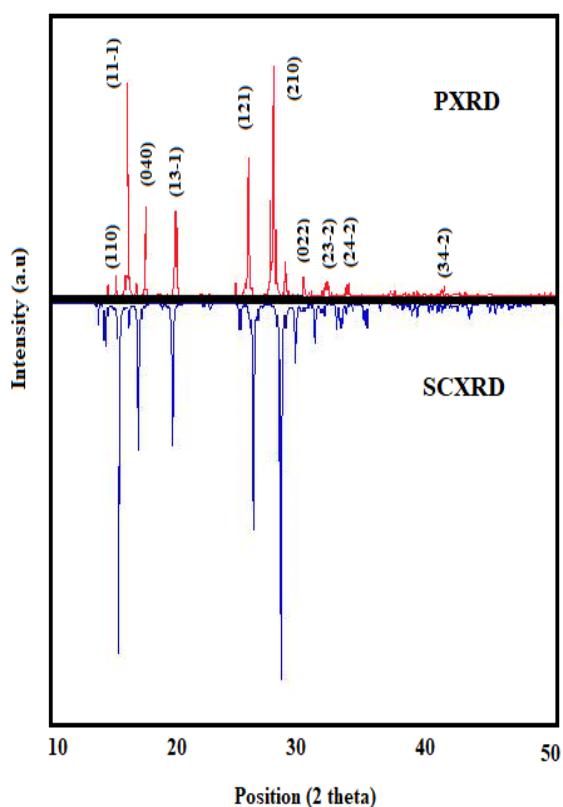


Figure 2. Comparison of SCXRD and PXRD data of 6AMP single crystal

3.2 FTIR spectral analysis

FTIR spectrum was used in the analyses of different functional groups and the vibrational frequencies present in the title compound. The analysis was performed through the KBr pellet method in the Mid IR region of 4000-500 cm^{-1} and given in Figure 3. The absorption band at 3600 cm^{-1} and 3250 cm^{-1} corresponds to the symmetric stretching vibration of OH and NH respectively. The peak at 2568 cm^{-1} , 2500 cm^{-1} , and 2328 cm^{-1} confirm the presence of NH wagging vibrations. The very strong (C=C) group indicates that the peak is at 1675 cm^{-1} . The peak at 1324 cm^{-1} belongs to the CH wagging vibration and CO wagging vibration. The peak at 1134 cm^{-1} attributes to the C-C symmetric stretching vibration. The CH scissoring vibrations are indicated by bands at 848 cm^{-1}

¹. Comparison of experimental and theoretical FTIR data are presented in Table.1

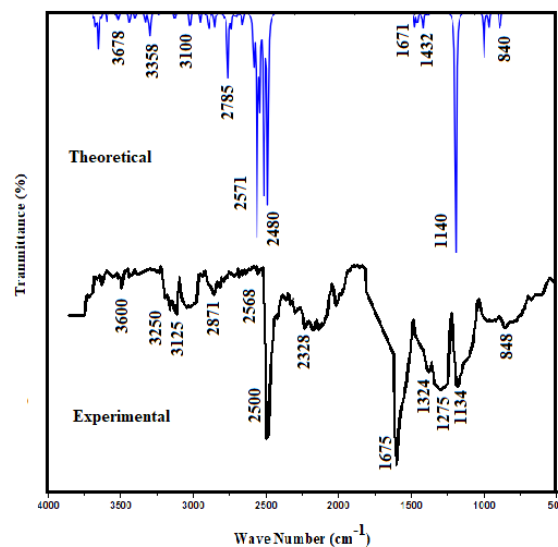


Fig 3. Comparison of experimental and theoretical FTIR spectrum of 6AMP single crystal

Table.1 Comparison of experimental and theoretical FT-IR and simulated band assignment of 6AMP

S.No	FTIR		Assignment with PED (%)
	Experimental	Theoretical	
1.	3600	3678	ν OH (99)
2.	3250	3358	ν NH(99)
3.	3125	3100	ν_{ass} CH (98)
4.	2871	2785	ω CH ₂ (96)
5.	2568	2571	ω NH (95)
6.	2500	2480	ω NH (82)
7.	2328	-	ω NH (47)
8.	1675	1671	ν C=C(88), ν CH(14)
9.	1324	1432	ω CH (28), ω CO (76)
10.	1134	1140	ν C-C (48)
11.	848	840	δ CH(15)

ν : Symmetry stretching, ν_{ass} : Assymetry stretching, ω : Wagging, and δ : Scissoring

3.3 UV-Vis NIR spectral analysis

The absorption studies were performed using a Perkin-Elmer Lambda-35 spectrophotometer for the grown crystal 6AMP. The measured optical transmittance spectrum was displayed in Figure.4 in the visible region of 200-800 nm. The spectral analysis of the crystal shows that the title compound has good transparency in the visible region with the maximum absorption at 215nm and 63% transmittance in the UV Visible region [17].

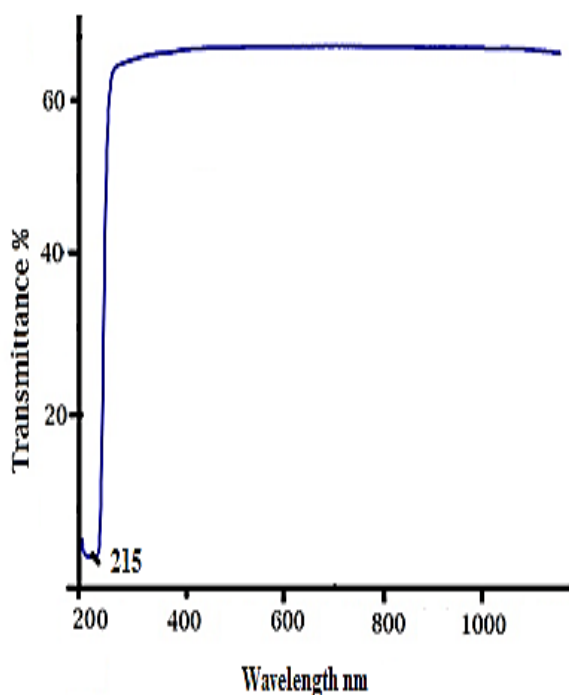


Fig 4. UV-Vis NIR spectrum of 6AMP single crystal

4. Computational details

Gaussian 09 program package was used for calculating the values theoretically such as electronegativity (χ), Chemical potential (μ), hardness (η), softness (S), and electrophilicity index (ω) which are the chemical descriptors and also the molecular structure was determined through HOMO – LUMO energy levels through B3LYP with 6-31G(d,p) basis sets.

The Electronegativity of the molecule is estimated as $(\chi) = \left(\frac{I+A}{2}\right)$

$$(1)$$

The chemical potential of the molecule approximated as, $\mu = -\left(\frac{I+A}{2}\right)$

$$(2)$$

The absolute hardness of the molecule is calculated as, $(\eta) = \frac{I-A}{2}$

$$(3)$$

The global softness (inverse of hardness) of the molecule evaluated as, $S = \frac{1}{2}\eta$

$$(4)$$

The value of the electrophilicity index determined as, $\omega = \frac{\mu^2}{2\eta}$

$$(5)$$

The nonlinear optical properties of the grown crystal were analyzed by the parameters which are as follows dipole moments (μ), polarizability (α), and the first-order hyperpolarizability (β) using the below equations:

$$\mu_{\text{tot}} = (\mu_x + \mu_y + \mu_z)^{1/2}$$

$$(6)$$

$$\alpha_{\text{tot}} = \frac{1}{3}(\alpha_{xx} + \alpha_{yy} + \alpha_{zz})$$

$$(7)$$

$$\beta = (\beta_x^2 + \beta_y^2 + \beta_z^2)^{1/2}$$

$$(8)$$

The equation for calculating the magnitude of first order hyper polarizability is given below:

$$\beta_{\text{tot}} = [(\beta_{xxx} + \beta_{xyy} + \beta_{xzz})^2 + (\beta_{yyy} + \beta_{yzz} + \beta_{yxx})^2 + (\beta_{zzz} + \beta_{zxx} + \beta_{zyy})^2]^{1/2} \quad (9)$$

The α_{tot} and β_{tot} values of Gaussian output are represented in (a.u) and therefore changed into electrostatic units (esu) (for α ; 1 a.u. = 0.1482×10^{-24} esu, for β ; 1 a.u. = 8.6393×10^{-33} esu).

Natural bond orbital (NBO) analyses were carried out by performed using NBO 3.1 program. The second-order Fock- matrix was performed to determine the donor (i) and acceptor (j) interaction on the NBO basis.

The stabilization energy $E^{(2)}$ for every donor (i) and acceptor (j) was given as:

$$E^{(2)} = q_i F(i,j)^2 / (\epsilon_j - \epsilon_i) \quad (10)$$

4.1 Frontier molecular orbital analysis

The frontier orbital gaps identified the kinetic stability of the molecule [18]. The frontier molecular orbital (FMO) helps to know about the conversion of the electron from the ground state to an excited state. Bandgap energy is the energy difference between the HOMO and LUMO levels. This energy difference determines the stability and reactivity of the molecule through the following parameters ionization potential (IP), electron affinity (EA), electronegativity (χ), hardness (η), softness (S), chemical potential (μ), and electrophilicity index (ω) anticipated for the grown 6AMP crystal are given in Table 2. Figure 5 depicts the HOMO-LUMO energy levels of a different state ($n \rightarrow \pi^*$ and $\pi \rightarrow \pi^*$ transitions). The ground-state band gap energy was calculated to be 5.25 eV.

Table 2: Calculated energy values of 6AMP

Basic set	B3LYP/6-311++G(d,p)
E_{HOMO} (eV)	-5.9877
E_{LUMO} (eV)	-0.7376
Ionization potential (IP)	5.9877
Electron affinity (EA)	0.7376
Energy gap (eV)	5.2501
Electronegativity (χ)	3.3627
Chemical potential (μ)	-3.3627
Chemical hardness (η)	2.6251
Chemical softness (S)	0.1905
Electrophilicity index (ω)	2.1538

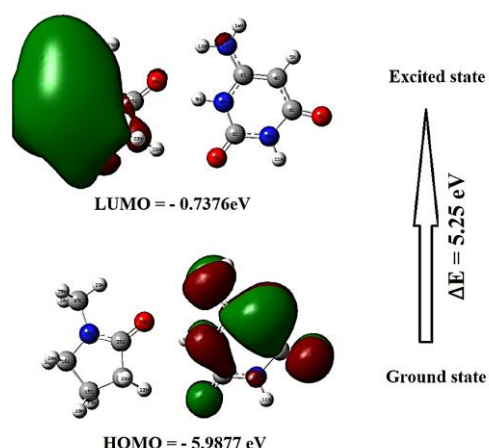


Figure.5. Frontier molecular orbital energy level diagram of 6AMP crystal at the B3LYP/6-311++G(d,p) in the gas phase.

4.2 Dipole Moment, Polarizability and Hyperpolarizability

The first hyperpolarizabilities (β) of this molecular device and associated properties (β , α_0 , and α) of 6AMP crystal was determined using B3LYP/6-311G++(d,p) basis sets. Table 3 lists the values of the electric dipole moment (Debye) and dipole moment components, polarizabilities, and hyperpolarizabilities of the 6AMP crystal. The total molecular dipole moment, polarizabilities and first hyperpolarizabilities are 10.6901 debye, 14.2774×10^{-24} esu and 3.062×10^{-30} esu in the B3LYP method with 6-311++G(d,p) levels of theory, which might become parable with the mentioned values of similar derivatives [19].

Table 3. The electric dipole moment (μ), polarizability (α_{Tot}) and hyper polarizability (β_{Tot}) at 6AMP crystal at B3LYP/6-311++G(d,p) methods.

Dipole moment (Debye)		Hyperpolarizability (a.u)	
Parameter	B3LYP/6-311++G(d,p)	Parameter	B3LYP/6-311++G(d,p)
μ_x	-10.2027	β_{xxx}	-329.2456
μ_y	3.0309	β_{yyy}	41.3344
μ_z	0.9983	β_{zzz}	-0.3177
μ	10.6901	β_{xyy}	10.6482
Polarizability (\AA^3)		β_{xxy}	17.5370
α_{xx}	-105.8456	β_{xxz}	-3.6313
α_{xy}	6.5166	β_{xzz}	-8.6955
α_{xz}	1.1917	β_{yzz}	-3.9162
α_{yy}	-87.7561	β_{yyz}	10.3253
α_{yz}	0.9424	β_{xyz}	9.6919
α_{zz}	-95.4149	β_{Tot}	3.062×10^{-30} esu
α_{Tot}	14.2774×10^{-24} esu		

and electron density distribution between atoms. The perturbation energies from the NBO analysis were given in Table 4. As concluded from the results of NBO, the strongest stabilization energies for the crystal 6AMP are defined as π (C1- C4) \rightarrow π^* (C3- O6) with energies of 28.60 at B3LYP. The important intramolecular hyper-conjugative interactions are:

n_2 (O6) \rightarrow σ^* (C3-C4), n_2 (O6) \rightarrow σ^* (C3-N10), n_2 (O7) \rightarrow σ^* (C2-N8), n_2 (O7) \rightarrow σ^* (C2-N10) with stabilization energies 16.27, 29.12, 23.75, 23.97 kJ/mol at B3LYP. The magnitudes of charge transfer from the lone pairs to anti-bonding interactions are: n_1 (N8) \rightarrow π^* (C1- C4), n_1 (N8) \rightarrow π^* (C2- O7), n_1 (N10) \rightarrow π^* (C2- O7), n_1 (N10) \rightarrow π^* (C3- O6), n_1 (N12) \rightarrow π^* (C1- C4) with stabilization energies 50.19, 56.74, 62.48, 45.60, 42.65 kJ/mol at B3LYP. In addition, the other high energy interactions between the anti-bonding π^* electrons of the carbonyl group to π^* (C1- C4) \rightarrow π^* (C3- O6) stabilizes the compound by stabilization energy of 222.51 kJ/mol.

4.3 Natural bond orbital (NBO)

NBO study was carried out at the B3LYP/6-311++G(d,p) theoretical levels of the 6AMP molecule in order to provide an explanation for intramolecular hybridization and delocalization of electron density within the molecule. In computational chemistry, natural bond orbital (NBO) is used to calculate bonds, donor-acceptor interactions, bond order

Table 4. Second-order perturbation theory analysis of Fock matrix in NBO basis of 6AMP crystal.

Donor(i)	Acceptor(j)	E(2) ^a (KJ mol ⁻¹)	E(i)-E(j) ^b (a.u)	F(i,j) ^c (a.u)
6-311++G(d,p)				
π C1-C4	π^* C3-O6	28.60	0.30	0.086
n2 O6	σ^* C3-C4	16.27	0.74	0.100
n2 O6	σ^* C3-N10	29.12	0.63	0.122
n2 O7	σ^* C2-N8	23.75	0.68	0.115
n2 O7	σ^* C2-N10	23.97	0.69	0.117
n1 N8	π^* C1-C4	50.19	0.29	0.108
n1 N8	π^* C2-O7	56.74	0.28	0.113
n1 N10	π^* C2-O7	62.48	0.27	0.117
n1 N10	π^* C3-O6	45.60	0.29	0.103
n1 N12	π^* C1-C4	42.65	0.31	0.106
π^* C1-C4	π^* C3-O6	222.51	0.01	0.073

more positive charge of 0.302384a.u. The nitrogen atoms N26 has a positive charge and N10, N12 possess a negative charge. Further, the theoretical analysis indicated that the oxygen atoms are additional electronegative compared to the carbon atoms by pulling the electrons for the formation of bonds between them. The 6AMP crystal contains the carbonyl oxygen atom and the hydroxyl hydrogen atoms, forming the functional groups. Electronic recombination occurs during hydrogen bond formation by transferring the charges between the atoms [20,21].

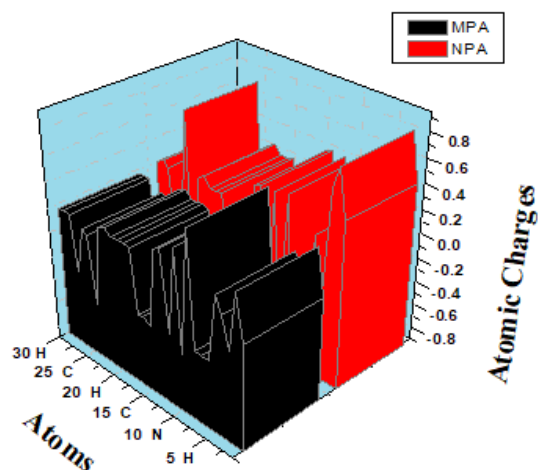


Figure.6 Mulliken population analysis and Natural population analysis

4.4 Mulliken population analysis and Natural population analysis

The natural atomic charge distribution and Mulliken population analysis (MPA) of 6AMP crystal were determined by the B3LYP/6-311++G(d,p) method and are presented in Figure 6. Table 5 shows the values of the natural atomic charge and the distribution of charge on various atoms (C, N, and O) from Mulliken population analysis (MPA) techniques. In this C2, C4, C17, C25 and C27 have a positive charge while the remaining carbon atoms have a negative charge. Carbon atoms the C2 carbon has a

Table 5. Mulliken Atomic Charge and Natural atomic charge of 6AMP

Atoms	6-311++G(d,p)	
	MPA	NPA
1 C	-0.062582	0.43934
2 C	0.302384	0.81445
3 C	-0.170802	0.64017
4 C	0.073039	-0.45255
5 H	0.184620	0.22630
6 O	-0.355921	-0.62979
7 O	-0.349392	-0.65977
8 N	-0.340058	-0.64540
9 H	0.568851	0.44467
10 N	-0.434844	-0.64618
11 H	0.359958	0.41504
12 N	-0.336332	-0.78247
13 H	0.309430	0.41133
14 H	0.266558	0.39085
15 C	-0.371320	-0.38981
16 C	-0.326813	-0.15462
17 C	-0.345932	-0.47777
18 H	0.167507	-0.21154
19 H	0.180880	0.20606
20 H	0.174014	0.18314
21 H	0.168294	0.19544
22 H	0.220634	0.26348
23 H	0.194224	0.22340
24 O	-0.469733	-0.71358
25 C	0.076674	0.71769
26 N	0.100899	-0.48540
27 C	-0.274806	-0.36061
28 H	0.161908	0.19183
29 H	0.171238	0.22773
30 H	0.157425	0.19549

4.5 Hirshfeld Surface analysis

Hirshfeld Surface (HS) analysis helps to observe the intermolecular interactions of the crystal structure. The normalized interaction distance (d_{norm}), shape index and

curvedness are computed as a result of the use of Crystal Explorer 3.1 and presented in Figure.7 (a-c). The d_{norm} is depending on the average values received from d_i and d_e . Here d_i represents the distance between Hirshfeld Surface and the adjoining atom inside the surface (red) and d_e is the distance between the Hirshfeld Surface and the nearby atom outside the surface (blue) [22]. The evident d_{norm} view, d_i and d_e are shown in Figure 8(a-c). Molecular interaction between the molecule was identified by 2D-fingerprint plots [23]. The 2D finger plots for the molecule 6AMP are displayed in figure 9. The molecular interaction between hydrogen-hydrogen (H...H) contacts contribution (inside to outside) is more (51.5%) while the oxygen-hydrogen (O...H) intermolecular interaction (14.6%) is the second maximum interaction. Other relative contribution of intermolecular interactions are H...O (11 %), C...H (5.9 %), H...C (4.1 %), N...H (4.1 %) and H...N (3.3 %).

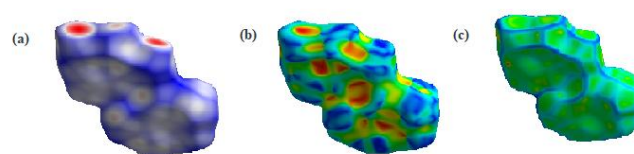


Figure.7 (a) Hirshfeld surfaces mapped with d_{norm} , (b) shape index, (c) curvedness

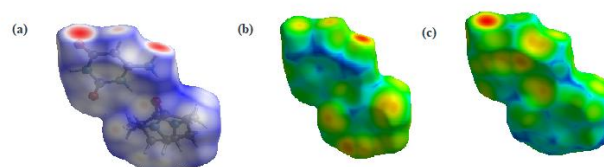


Figure.8 Hirshfeld surfaces mapped with (a) d_{norm} (transparent view), (b) d_i , (c) d_e

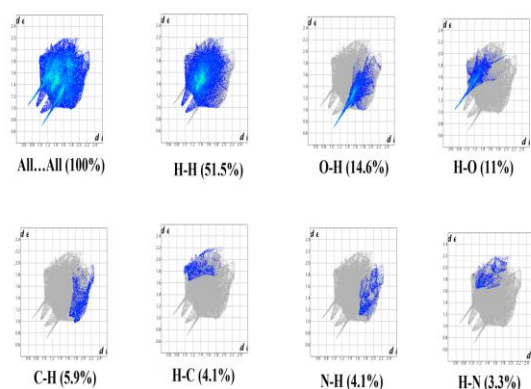


Figure. 9 Fingerprint plots of interactions between the various elements

6. Conclusion

In summary, 6AMP single crystal was grown by slow evaporation solution growth technique at normal ambient temperature. Single X-ray diffraction analysis was used for the confirmation of lattice parameters. The crystalline planes and their purity were observed through PXRD. The functional groups present in the compound 6AMP were analyzed by FTIR spectral analysis. The crystal transparency was found in the entire visible region with the absorption wavelength at 215nm from UV-vis-NIR spectral analysis. The HOMO-LUMO energy gap of the grown crystal 6AMP at B3LYP/6-311G++ (d,p) is 5.25 eV. The Density functional theory determined for the 6AMP crystal compound would possibly have macroscopic first hyperpolarizability with non-zero values acquired by the numerical second derivatives of the electric dipole moment with respect to the applied field strength. The intermolecular interactions existing in the crystal were analyzed by Hirshfeld surface analysis.

Conflict of interest:

The authors declare no conflict of interest with this work.

Acknowledgment

One of the authors (RS) thanks the Tamil Nadu State Council for Higher Education and Tamil Nadu State Council for Science and Technology, Chennai, Tamil Nadu, India for the financial support [File No. D.O.Rc.No.744/2017 A and TNSCST/STP/AR/PS/2014-15, Date: 11.04.2017]. Authors thank IIT Madras, Chennai, for extending laboratory facilities to record the FT-IR spectrum. The authors thank CECRI, Karaikudi, and Sastra University, Thanjavur, for extending the laboratory facilities to record the Powder XRD spectrum respectively.

References

1. Z. Moradi-Shoeili, Z. Amini, D. M. Boghaei, and B. Notash, "Synthesis, X-ray structure and ascorbic oxidation properties of ternary α -amino acid Schiff base-bipyCu(II) complexes as functional models for ascorbic oxidase," *Polyhedron*, vol. 53, pp.76–82, 2013.
2. Preeti Singh, MM Abdullah, Suresh Sagadevan, SaiqaIkram, *J Mater Sci: Mater Electron*, 29 (2018) 7904–7916
3. A. R. Patil, K. J. Donde, S. S. Raut, V. R. Patil, and R. S. Lokhande, "Synthesis, characterization and biological activity of mixed ligand Co(II) complexes of schiff base 2-amino-4-nitrophenoln-salicylidene with some amino acids," *Journal of Chemical and Pharmaceutical Research*, vol. 4, no. 2, pp. 1413–1425, 2012.
4. Z. S. M. Al-Garawi, I. H. R. Tomi, and A. H. R. Al-Daraji, "Synthesis and characterization of new amino acid-schiff bases and studies their effects on the activity of ACP, PAP and NPA enzymes (*In Vitro*)," *E-Journal of Chemistry*, vol. 9, no. 2, pp. 962–969, 2012.
5. F. Ciolan, L. Patron, G. Marinescu, N. Cioatera, and M. Muresanu, "Synthesis and

- characterization of Zn(II) binuclear complexes with three schiff bases derived from some aminoacids and 2,2□-(propane-1,3-diylldioxy)dibenzaldehyde,” *Revistade Chimie*, vol. 62, no. 12, pp. 1145–1149, 2011.
6. P. R. Reddy, A. Shilpa, N. Raju, and P. Raghavaiah, “Synthesis, structure, DNA binding and cleavage properties of ternary amino acid Schiff base-phen/bipy Cu(II) complexes,” *Journal of Inorganic Biochemistry*, vol. 105, no. 12, pp. 1603–1612, 2011.
 7. Baraniraj, T., Philominathan, P., *Spectrochim. Acta Part A*. (2010). 75, 74-76.
 8. G.L. Patrick, *An introduction to Medicinal Chemistry*, Oxford University Press, 2001.
 9. W. B. Parker, *Chem. Rev.*, 2009, 109, 2880-2893.
 10. N. Tolstoluzhsky, P. Nikolaienko, N. Gorobets, E.V. Van der Eycken and N. Kolos, *Eur. J. Org. Chem*, 2013, 5364-5369.
 11. N. Tolstoluzhsky, P. Nikolaienko, N. Gorobets, E.V. Van der Eycken and N. Kolos, *Eur. J. Org. Chem*, 53 (2013)64-5369.
 12. R. Edupuganti, Q. Wang, C.D.J. Tavares, C.A. Chitjian, J.L. Bachman, P. Ren, E.V Anslyn and K.N. Dalby, *Bioorg. Med. Chem.* 22 (2014) 4910-4916.
 13. A. Palasz and D. Ciez, *Eur. J. Med. Chem.*, 97 (2015)582-611.
 14. P. J. Parsons, C.S. Penkett and A.J. Shell, *Chem. Rev.*, 96 (1996) 195-206
 15. N.T. Jui, J.A.O. Garber, F.G. Finelli, D.W.C. MacMillan, *J. Am. Chem. Soc.* 134 (2012) 11400-11403
 16. Valeska Gerhardt., and Michael Bolte., *Acta Cryst.* (2013). C69 (2013) 1402-1407.
 17. C. N. R. Rao, *Ultraviolet And Visible Spectroscopy of organic Compound*, Prentice Hall., Pvt., Ltd., New Delhi, (1984)
 18. Muthu, K., Meenatchi, V., Rajasekar. M., Prasad, A.A., Meena, K., Agilandeshwari, R., Kanagarajan, V., Meenakshisundaram, S.P., J. *Mol. Struct.* 1091(2015) 210-221.
 19. Raja, M., Muhamed, R.R., Muthu, S., Suresh, M., *J. Mol. Struc.* 1141 ((2017)284-298.
 20. M. Karabacak, L. Sinha, O. Prasad, Z. Cinar, M. Cinar, *Spectrochim. Acta*, 93 (2012)33–46.
 21. Steiner, T., *The hydrogen bond in the solid-state*, *Angew. Chem. Int. Ed.* 41 (2002) 48-76.
 22. Patel, D.K., Patel, U.H. *J. Mol. Struct.* 1128 (2017)127-134.
 23. Spackman, M.A., and McKinnon, J.J., *CrystEngComm*. 4(2002) 378-392.
- [1] P.N. Prasad, D.J. Williams, *Introduction to Nonlinear Optical Effects in Organic Molecules and Polymers*, Wiley, New York, 1991
- [2] Z. Moradi-Shoeili, Z. Amini, D. M. Boghaei, and B. Notash, “Synthesis, X-ray structure and ascorbic oxidation properties of ternary α -amino acid Schiff base-bipy Cu(II) complexes as functional models for ascorbic oxidase,” *Polyhedron*, vol. 53, pp. 76–82, 2013.
- [3] A. R. Patil, K. J. Donde, S. S. Raut, V. R. Patil, and R. S. Lokhande, “Synthesis, characterization and biological activity of mixed ligand Co(II) complexes of schiff base 2-amino-4-nitrophenol-n-salicylidene with some amino acids,” *Journal of Chemical and Pharmaceutical Research*, vol. 4, no. 2, pp. 1413–1425, 2012.
- [4] Z. S. M. Al-Garawi, I. H. R. Tomi, and A. H. R. Al-Daraji, “Synthesis and characterization of new amino acid-schiff bases and studies their effects on the activity of ACP, PAP and NPA

enzymes (*In Vitro*)," *E-Journal of Chemistry*, vol. 9, no. 2, pp.962–969, 2012.

[5] F. Ciolan, L. Patron, G. Marinescu, N. Cioatera, and M.Mureseanu, "Synthesis and characterization of Zn(II) binuclear complexes with three schiff bases derived from some aminoacids and 2,2□-(propane-1,3-diyldioxy)dibenzaldehyde," *Revistade Chimie*, vol. 62, no. 12, pp. 1145–1149, 2011.

[6] P. R. Reddy, A. Shilpa, N. Raju, and P. Raghavaiah, "Synthesis, structure, DNA binding and cleavage properties of ternary amino acid Schiff base-phen/bipy Cu(II) complexes," *Journal of Inorganic Biochemistry*, vol. 105, no. 12, pp. 1603–1612, 2011.

[7] Baraniraj, T., Philominathan, P., *Spectrochim. Acta Part A*. (2010). 75, 74-76.

[8] G.L. Patrick, *An introduction to Medicinal Chemistry*, Oxford University Press, 2001.

[9] W. B. Parker, *Chem. Rev.*, 2009, 109, 2880-2893.

[10] N. Tolstoluzhsky, P. Nikolaienko, N. Gorobets, E.V. Van der Eycken and N. Kolos, *Eur. J. Org. Chem*, 2013, 5364-5369.

[11] R. Edupuganti, Q. Wang, C.D.J. Tavares, C.A. Chitjian, J.L. Bachman, P. Ren, E.V. Anslyn and K.N. Dalby, *Bioorg. Med. Chem.* 2014, 22, 4910-4916.

[12] A. Palasz and D. Ciez, *Eur. J. Med. Chem.*, 2015, 97, 582-611.

[13] P. J. Parsons, C.S. Penkett and A.J. Shell, *Chem. Rev.*, 1996, 96, 195-206

[14] N.T. Jui, J.A.O. Garber, F.G. Finelli, D.W.C. MacMillan, *J. Am. Chem. Soc.* 134 (2012) 11400-11403